

# Flow-Bench: A Dataset for Computational Workflow Anomaly Detection

**George Papadimitriou\***

University of Southern California  
Los Angeles, CA  
georgpap@isi.edu

**Hongwei Jin\***

Argonne National Laboratory  
Lemont, IL  
jinh@anl.gov

**Cong Wang**

RENCI  
Chapel Hill, NC  
cwang@renci.org

**Krishnan Raghavan**

Argonne National Laboratory  
Lemont, IL  
kraghavan@anl.gov

**Anirban Mandal**

RENCI  
Chapel Hill, NC  
anirban@renci.org

**Prasanna Balaprakash**

Oak Ridge National Laboratory  
Oak Ridge, TN  
pbalapra@ornl.gov

**Ewa Deelman**

University of Southern California  
Los Angeles, CA  
deelman@isi.edu

## Abstract

A computational workflow, also known as workflow, consists of tasks that must be executed in a specific order to attain a specific goal. Often, in fields such as biology, chemistry, physics, and data science, among others, these workflows are complex and are executed in large-scale, distributed, and heterogeneous computing environments that are prone to failures and performance degradations. Therefore, anomaly detection for workflows is an important paradigm that aims to identify unexpected behavior or errors in workflow execution. This crucial task to improve the reliability of workflow executions must be assisted by machine learning-based techniques. However, such application is limited, in large part, due to the lack of open datasets and benchmarking. To address this gap, we make the following contributions in this paper: (1) we systematically inject anomalies and collect raw execution logs from workflows executing on distributed infrastructures; (2) we summarize the statistics of new datasets, as well as a set of open datasets, and provide insightful analyses; (3) we benchmark unsupervised anomaly detection techniques by converting workflows into both tabular and graph-structured data. Our findings allow us to examine the effectiveness and efficiencies of the benchmark methods and identify potential research opportunities for improvement and generalization. The dataset and benchmark code are available online with MIT License for public usage.

## 1 Introduction

Computational workflows that run on distributed and parallel computing environments, such as Southern California Earthquake Center’s (SCEC) Cybershake [Callaghan et al., 2014] and LIGO’s PyCBC [Nitz et al., 2017], have become an integral part of scientific, engineering, and data science research, enabling the simulation and modeling of complex otherwise impossible complex phenomena.

---

\*Equal contribution

However, in recent years, the scale and complexity of computational workflow systems have increased significantly. This increase has made these workflow applications prone to various types of hardware and software faults, including performance anomalies, crashes, and security breaches. These faults can cause significant disruptions to high-performance computing (HPC) applications, resulting in lost productivity, wasted resources, and potentially serious consequences for scientific discoveries.

To address this challenge, anomaly detection has emerged as a promising approach for detecting and diagnosing faults in workflows. Anomaly detection refers to the process of identifying patterns or behaviors that deviate significantly from expected (or normal) behavior. Detection of anomalies enables system administrators and users to take proactive measures to prevent or mitigate the impact of faults, improving the overall reliability and efficiency of the workflow. In recent years, various research efforts have been devoted to developing and evaluating anomaly detection techniques for computational workflows. While anomaly detection in workflows is very desirable, key challenges still persist: (1) there is no template for determining the relevance of deviations in the workflow settings, (2) most of the time, the training data is comprised of several orders of magnitude more data points corresponding to the normal than the anomaly, and (3) more often than not, labeling the anomalies in workflows incurs a lot of time and effort.

These fundamental challenges make the anomaly detection problem hard. Although standard anomaly detection benchmarks such as Zhao et al. [2019b] and Liu et al. [2022] can be applied to workflows as is shown in this paper, these methods are not very effective and do not scale well with the size of the workflow as well. Specifically, we show in section 4 that many readily available anomaly detection methods result in out-of-memory (OOM) errors when encountering simple workflow data. On the other hand, the methods that do manage to work on the workflow data, do not provide desirable precision. Moreover, there is still a lack of consensus on the best practices and benchmark datasets that facilitate the evaluation of different anomaly detection techniques on computational workflows making it difficult to compare and reproduce the results of different studies.

These challenges indicate the need for careful analysis and study of workflow data but the benchmarks needed for such analysis on workflows are not available in the literature. In this work, we present a set of novel workflows along with best practices and preliminary analysis that will provide the tools for future research to test and develop tools to facilitate anomaly detection on workflows. In particular, we present a benchmark study of anomaly detection techniques for workflows. We introduce a set of new workflow data that we have collected for anomaly detection and evaluate the performance of several state-of-the-art anomaly detection techniques, including tabular data anomaly detection [Zhao et al., 2019b] and graph data anomaly detection [Liu et al., 2022]. We evaluate the performance of several state-of-the-art anomaly detection techniques on a range of high-throughput workloads and datasets, including simulation, data analysis, and machine learning applications. Our evaluation is based on unsupervised learning with several performance metrics, including ROC-AUC score, F1-score, top-k score and etc. We compare strengths and weaknesses of different anomaly detection techniques and reveal insights into their applicability and limitations in scientific workflow scenarios.

In spite of our benchmark being focused on computational workflows, it is important to note that, challenges such as non-stationarity in input data distribution, differences in the number of nodes and features, the size of the data, and especially the lack of labels, provide a real-world example that can be readily utilized for the development of anomaly detection tools for the larger ML community. In contrast, popular benchmark tools such as PyOD [Zhao et al., 2019b] and PyGOD [Liu et al., 2022] do not provide these unique features.

## 1.1 Contributions

We introduce a set of workflow data that allow the careful study and development of novel anomaly detection approaches for computational workflows. We provide a comprehensive study to demonstrate the utility of our data with already available benchmarks and why novel methods are necessary.

## 2 Related Works

There are several techniques that have been proposed for anomaly detection. Statistical methods, machine learning (ML) methods, rule-based methods, and hybrid methods are the four major categories of these methods. Statistical methods formulate the anomaly detection problem as the detection

of outliers in a distribution and therefore, methods such as clustering [Sohn et al., 2023], principal component analysis (PCA) [Ma et al., 2023], and auto-regressive integrated moving average (ARIMA) models [Goldstein, 2023] are commonly utilized. On the other hand, the ML methods involve learning a classifier map between the anomaly class and the input data. These methods have been developed for both tabular and graph data and popular methods include (graph) neural networks [Yuan et al., 2021], decision trees [Breiman, 2001], and support vector machines (SVMs) [Schölkopf et al., 2001]. Hybrid methods take the probabilistic efficiency of statistical methods and combine it with the ability of ML methods to characterize complex distribution to improve the accuracy and robustness of anomaly detection [Kriegel et al., 2008].

Another class of anomaly detection methods involves rule-based methods or expert systems where a set of rules must be defined to characterize normal system behavior. These rules can then be used to detect anomalies [Liu et al., 2008] in the data. These rules can either be based on expert knowledge or derived from historical data or ML or probabilistic models that encode normal information.

While a non-exhaustive list of anomaly detection methods is presented above, all these methods can be potentially used in workflows. However, it is important to note that the choice of technique(s) for anomaly detection in workflows depends on the specific requirements and characteristics of the system being monitored, as well as the goals of the anomaly detection. For instance, a graph neural network (GNN)-based approach is more suitable for workflows than methods designed for tabular data, because the dependency structure present in workflow data is rather important to characterize anomalies in computational workflows. Furthermore, computational workflows are unique in the setup as each workflow differs in the number of jobs, the dependency graph, and other structures. While training a separate anomaly detection approach for each of the workflow is not efficient, typical approaches that are discussed above except the graph neural network-based are not really suitable when the input data dimensions change for every computational workflow. On the other hand, workflow data can be rather large, and complex ML-based approaches run out of memory when trying to detect anomalies in these datasets.

In the past, datasets containing system logs of large systems (e.g., BlueGene, Thunderbird) have been released to the community Oliner and Stearley [2007], however, these logs are unstructured and they don't match the statistics and events to the workloads that were executed on these systems. Providing a dataset that offers a direct correlation between system logs and the workflow application is important in creating new ML methods that better capture and identify workflow anomalies.

### 3 Dataset

The datasets used for benchmarking anomaly detection in computational workflows should be representative of the types of data encountered in real applications. The datasets should include both normal and anomalous data to evaluate the performance of the base method. Some important statistics that should be considered when selecting datasets are:

- **Data size:** The dataset should be large enough to capture the variability in the data, but not so large that it becomes computationally impractical to analyze and benchmark.
- **Data dimensionality:** The number of features or variables in the dataset should be representative of the types of data encountered in real applications.
- **Data distribution:** The dataset should represent the typical distribution of the data encountered in real applications.

#### 3.1 Workflow Applications

Towards this end, we choose three workflow applications that are unique in their characteristics and are representative of real-world applications.

##### 3.1.1 1000 Genome Workflow

The 1000 genome project [1000 Genomes Project Consortium, 2012] provides a reference for human variation, having reconstructed the genomes of 2,504 individuals across 26 different populations. The test case we have here, identifies mutational overlaps using data from the 1000 genomes project in order to provide a null distribution for rigorous statistical evaluation of potential disease-related

mutations. This workflow (Figure 3 in Appendix A) is composed of five different tasks: (1) individuals – fetches and parses the Phase 3 data from the 1000 genomes project per chromosome; (2) populations – fetches and parses six populations (African, Mixed American, East Asian, European, South Asian, and British) and a set of all individuals; (3) sifting – computes the SIFT scores of all of the SNPs (single nucleotide polymorphisms) variants, as computed by the Variant Effect Predictor; (4) pair overlap mutations – measures the overlap in mutations (SNPs) among pairs of individuals; and (5) frequency overlap mutations – calculates the frequency of overlapping mutations across sub-samples of certain individuals.

### 3.1.2 Montage Workflow

Montage is an astronomical image toolkit [Jacob et al., 2010] with components for re-projection, background matching, co-addition, and visualization of FITS files. Montage workflows typically follow a predictable structure based on the inputs, with each stage of the workflow often taking place in discrete levels separated by some synchronization/reduction tasks (mConcatFit and mBgModel). The workflow (Figure 4 in Appendix A) uses the Montage to transform astronomical images into custom mosaics, and is composed of eight different tasks: (1) mProject – re-projects infrared images using a predefined target projection; (2) mDiffFit – calculates the difference between a single pair of overlapping images; (3) mConcatFit – merges multiple plane FITS files into a single file; (4) mBgModel – uses the image-to-image differences and selects a set of corrections to be applied; (5) mBackground – applies the background correction to each of the images; (6) mImgTbl – extracts the FITS header geometry information and creates an ASCII image metadata table; (7) mAdd – co-adds the re-projected images to form a mosaic and populates the FITS header keywords; (8) mViewer – takes a FITS file and generates a gray-scale JPEG image. To generate a color JPEG image, the workflow is typically configured to map images from the bands the telescope collected the data, such as infrared, to the red, green, and blue bands visible to humans. As expected, Montage workflows are I/O bound, and total data footprints can range up to hundreds or thousands of gigabytes.

### 3.1.3 Predict Future Sales (Data Science) Workflow

The predict future sales workflow provides a solution to Kaggle’s predict future sales competition [Kaggle, 2020]. The workflow receives daily historical sales data from January 2013 to October 2015 and attempts to predict the sales for November 2015. The workflow includes multiple pre-processing and feature engineering steps to augment the dataset with new features and separates the dataset into three major groups based on their type and sales performance. To improve the prediction score, the workflow goes through a hyperparameter tuning phase and trains 3 discrete XGBoost models for each item group. In the end, it applies a simple ensemble technique that uses the appropriate model for each item prediction and combines the results into a single output file. Figure 5 in Appendix A presents the predict future sales workflow, which is composed of eleven different tasks: (1) Preprocess – performs data cleanup and removes outliers; (2) Feature Eng. X – each of these tasks extends the dataset by creating new features, using the currently available ones; (3) Features NLP – creates word embeddings and adds new features that can be used to cluster similar items together, based on their names; (4) Merge Features – merges all features, splits the items into 3 distinct groups and separates the dataset into training and test sets; (5) Generate HP Tuning SubWorkflow – generates a hyperparameter tuning subworkflow, where each task is testing a different set of features; (6) HP Tuning Workflow – submits and monitors the execution of the subworkflow; (7) XGBoost HP Tuning Conf. X – each of these tasks considers a different set of features and uses Hyperopt [Bergstra et al., 2013] to tune the XGBoost [Chen et al., 2015] model parameters, the number of tasks is configurable based on how many feature combinations we want to test; (8) Best XGBoost Params – compares the results of each hyperparameter tuning round and picks the best parameters; (9) Train XGBoost Model – trains the XGBoost model with the best parameters found; (10) Predict Sales – performs the sales prediction using the trained XGBoost model; (11) Merge Predictions – combines the predictions of all groups together in a single file.

## 3.2 Data Collection

To execute the workflows described in Sections 3.1.1, 3.1.2, 3.1.3, manage their execution and collect events and statistics, we used the Pegasus Workflow Management System (WMS) [Deelman et al., 2015].

### 3.2.1 Workflow Model

In Pegasus, workflows are represented as Directed Acyclic Graphs (DAGs), where nodes represent jobs, and edges represent sequential dependencies and data dependencies between the jobs. A job can only be submitted when all its dependencies have been met. For a more formal definition, a workflow is described as a DAG  $\mathcal{G} = (\mathcal{V}, \mathcal{E})$ , where  $\mathcal{V} = \{v_1, \dots, v_n\}$  represents the set of  $n$  jobs and  $\mathcal{E} \subseteq \mathcal{V}^2$  represents data dependencies between jobs. If  $e_{ij} = (v_i, v_j) \in \mathcal{E}$ , job  $v_i$  must complete its execution before  $v_j$  can start. We define  $\text{succ}(v_i) = \{v_k \mid (v_i, v_k) \in \mathcal{E}\}$  (resp.  $\text{pred}(v_i) = \{v_k \mid (v_k, v_i) \in \mathcal{E}\}$ ) to be the successors (resp. predecessors) of the job  $v_i \in \mathcal{V}$ . A job ( $v_i$ ) of a Pegasus workflow can be classified into one of these three categories: (1) *Compute* jobs describe computational tasks; (2) *Transfer* jobs move data to and from an execution site/node; (3) *Auxiliary* jobs create working directories, clean up unused data or perform other Pegasus internal bookkeeping tasks.

Additionally, Pegasus collects provenance data and events during the execution of a workflow and associates them with the jobs that produced them. The Pegasus Panorama extensions [Deelman et al., 2017, SciTech, 2017, Papadimitriou et al., 2021] enhance the workflow DAG with features containing execution metrics and infrastructure statistics per job ( $v_i$ ). These extensions enable the collection of execution traces of computational tasks, the collection of statistics of individual data transfers, the collection of infrastructure-related metrics, and all of them are stored in an Elasticsearch instance [ELK Stack, 2018].

### 3.2.2 Execution Infrastructure

To facilitate the workflow execution, we provisioned resources at the NSF Chameleon Cloud [Keahey et al., 2020]. We provisioned 4 Cascade Lake bare-metal nodes (48 Cores and 192GB RAM), where 1 had the role of *submit node* and 3 had the role of *Docker container executor nodes* [Docker Inc., 2022]. The container executor nodes were located within the same Chameleon region (Texas Advanced Computing Center - TACC), while the submit node was located at the University of Chicago region, and the connectivity between the two regions was established over a high-speed layer 2 VLAN (10 Gbps). On our *submit node* we configured an Apache HTTP server, we installed the Pegasus WMS [Deelman et al., 2015] binaries to manage the workflow execution, and we installed and configured HTCondor [HTCondor, 2023] to manage the baremetal resources we had provisioned.

To create an HTCondor pool of resources, we spawned HTCondor’s Executor containers on the Docker nodes, and in the case of the 1000 Genome and the Montage workflows, we created 20 containers with 4 cores and 16GB RAM each, while for the Predict Future Sales workflow, we created 18 containers with 8 cores and 32GB RAM each. For the latter, we assigned more resources to each executor container to accommodate the hyper-parameter optimization phase, which leverages multiple cores and demands more memory. Core and RAM resources were mapped to the containers using Docker’s runtime options (cpuset, memory). To deliver data to the executor containers we used the *submit node*’s HTTP server and we capped the download and upload speed to 1Gbps per HTCondor Executor container.

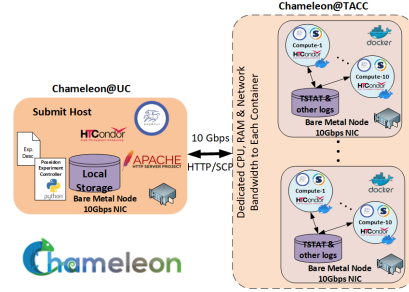


Figure 1: Overview of the execution infrastructure.

### 3.2.3 Synthetic Anomalies

To introduce synthetic anomalies, we used Docker’s runtime options to limit and shape the performance of the spawned container executor nodes. Through the runtime options, we were able to configure the amount of CPU time an executor container is allotted and limit the average I/O each executor container can perform. These capabilities are supported via Linux’s control groups version 2 [Kernel, 2015]. This approach offers sufficient isolation among the executors and allows us to obtain reproducible results from each type of experiment.

## 3.3 Dataset Description

Table 1 presents statistics of the executable workflow DAGs on the Chameleon provisioned resources. Throughout the data harvesting phase, we maintained the DAGs of the three workflows unchanged,

Table 1: Overall Dataset Statistics. We label the nodes as Normal, CPU  $K$  and HDD  $K$ .

Normal: No anomaly is introduced – normal conditions.

CPU  $K$ :  $M$  cores are advertised, but on some nodes,  $K$  cores are not allowed to be used. ( $K = 2, 3, 4$   $M = 4, 8$  and  $K < M$ )

HDD  $K$ : On some executor nodes, the average write speed to the disk is capped at  $K$  MB/s and the read speed at  $(2 \times K)$  MB/s. ( $K = 5, 10$ )

| Workflow             | DAG Information |       | #DAG Executions |     |    |    |     |    | #Total Nodes per Type |      |       |      |      |       |
|----------------------|-----------------|-------|-----------------|-----|----|----|-----|----|-----------------------|------|-------|------|------|-------|
|                      | Nodes           | Edges | Normal          | CPU |    |    | HDD |    | Normal                | CPU  |       |      | HDD  |       |
| 1000 Genome          | 137             | 289   | 51              | 100 | 25 | -  | 100 | 75 | 32398                 | 5173 | 756   | -    | 5392 | 4368  |
| Montage              | 539             | 2838  | 51              | 46  | 80 | -  | 67  | 76 | 137229                | 4094 | 11161 | -    | 8947 | 11049 |
| Predict Future Sales | 165             | 581   | 100             | 88  | 88 | 88 | 88  | 88 | 72609                 | 3361 | 3323  | 3193 | 3321 | 3293  |

and the DAG information presented in Table 1 reflects the number of nodes and edges of the final executable workflow DAGs submitted by Pegasus. The dataset contains over 1200 workflow executions, under normal and 2 anomalous conditions, with different anomaly levels. By using the method of Section 3.2.3 to inject synthetic anomalies, the anomalies are introduced on a per DAG node level, and as a result, each DAG execution can have a different set of anomalous nodes, since HTCondor negotiates which worker will accept a job at submission time. The dataset contains 6 tags *normal*, *cpu\_2*, *cpu\_3*, *cpu\_4*, *hdd\_5* and *hdd\_10*, that label the DAG nodes appropriately. Finally, the dataset provides the raw logs generated by Pegasus WMS and our experimental harness, and a parsed version, where we combined the raw logs into a single log file for each DAG execution. In the raw data we are offering (1) the workflows and the configurations used to execute them; (2) the original workflow submit directories of all DAG executions; (3) the workflow management system logs; (4) an experiment log file mapping the workflow DAG executions to the injected anomalies; (5) provenance data of each job, gathered by the WMS; (6) an Elasticsearch instance with all the captured workflow events, transfer events and resource utilization traces. Since we acquired the logs and metrics using an ephemeral private cloud instance, there is no sensitive information included in the dataset. The total size of the raw logs is approx. 39GB.

### 3.3.1 Parsed Data



Figure 2: Combining the raw logs to create a single CSV log file.

To generate the parsed version of the dataset, we combined information coming from the executable DAGs, the experiment log containing the anomaly labels, Pegasus’ logs, and the events hosted in Elasticsearch (Figure 2). During parsing, a CSV log file gets generated for every workflow DAG execution and is saved under the corresponding anomaly folder. The features present in the parsed data are listed in Table 3 in the appendix with their corresponding description, and the total size of the parsed data is 158MB. All of our assets will be released under the MIT License.

## 4 ML Benchmarks on Computational Workflows

Anomaly detection in computational workflows is an essential task to ensure that experimental results are reliable and reproducible. A benchmark for anomaly detection in computational workflows would require selecting appropriate baseline methods, and various metrics to evaluate the performance.

The baseline methods for anomaly detection can be broadly classified into supervised learning and unsupervised based on the availability of labels in our workflows.

**Supervised learning.** Supervised anomaly detection models are trained on labeled data, where the job anomalies are already known. These models learn to identify anomalies based on the labeled data and can be used to detect anomalies in new, unlabeled data. Exemplified classical methods are: support vector machine (SVM) [Hearst et al., 1998], decision trees [Quinlan, 1986], random forest [Breiman, 2001], etc. Specific to the DAGs, there are (semi)supervised learning algorithms that can learn the structural and feature information simultaneously, such as GraphSAGE [Hamilton et al., 2017], GAT [Velivckovic et al., 2018], etc.

On the other hand, it is usually the case labels corresponding to the anomalies that are unavailable, hard, and/or impossible to obtain. In this case, we usually turn to unsupervised learning methods. As this is the case with workflow data, unsupervised learning is the primary focus of the work.

**Unsupervised learning.** Unsupervised anomaly detection models do not rely on labeled data and instead look for patterns or data points that are significantly different from the rest of the data. These methods are useful when it is difficult or impossible to obtain labeled data, which is typically the case in computational workflows. Exemplified methods like: clustering (*e.g.*, k-means [Lloyd, 1982]), density-based methods (*e.g.*, k-nearest neighbors [Ramaswamy et al., 2000]), generative models (*e.g.*, auto-encoder [Sakurada and Yairi, 2014]), etc. In this work, we adopt the methods from PyOD [Zhao et al., 2019b], where the data are considered as tabular data, and PyGOD [Liu et al., 2022], where the data are considered as structural data, as benchmarks, reporting a set of metrics, and provide insightful analysis of the data we collected. Table 4 in appendix C provides a set of selected algorithms with their details.

**Benchmarking setup.** We began by converting our parsed data from Section 3.3.1 into a PyTorch Geometric (PyG) dataset [Fey and Lenssen, 2019]. PyG is widely used for graph data and can be converted to PyTorch and Numpy tabular format for convenience in adapting existing models. We then normalized the datasets column-wise (feature) and aligned the timestamps. Finally, we randomly split the data into training, validation, and testing sets with a ratio of 3:1:1, either in graph data format or tabular data format. A detailed data processing is provided in appendix D.

The experiments were conducted on a single machine that featured two Intel Xeon Gold 5317 processors, 256GB of local RAM, and an NVIDIA A30 GPU with a capacity of 24GB RAM. Because of the different backend implementations using either Scikit-learn or PyTorch, we give priority to using the CPU with the assistance of the GPU when the training process takes too long. More detailed hyperparameter setups of each algorithm are included in appendix E.

**Metrics and benchmark results.** Unsupervised learning involves training models on unlabeled datasets to identify anomalies without explicit guidance. Table 1 shows that the binary labels in the dataset are imbalanced. Therefore, performance is evaluated using metrics such as ROC-AUC, average precision, and top-k precision scores, in which we initially set the value of  $k$  to the number of true anomalies in the test set.

We evaluate the three novel workflows that we have introduced in this work with all the different unsupervised learning methods. We summarize the performance metrics discussed above in Table 2. However, many of the deep learning methods encounter out-of-memory (OOM) and time-limit-exceed (TLE) errors when applied to the 1000 Genome and Montage datasets. The inefficiency in handling large sizes of workflows is mainly attributed to the complexity of the operations involved in methods such as graph completion and reconstruction, which operate on sparse graphs. These methods encounter difficulties in dealing with the large sizes typically found in datasets like the 1000 Genome and Montage, thereby leading to errors.

Furthermore, it is observed that deep learning methods, aided by an additional input from the structure, denoted as  $A$  in Table 4, exhibit improved results relative to traditional statistical methods. For instance, the GCNAE algorithm for the 1000 Genome workflow, and Radar for Predict Future Sales workflow demonstrate better performance. Moreover, despite better performance, the precision achieved by these approaches is unsatisfactory. However, to effectively apply deep learning methods for anomaly detection, it is crucial to carefully design algorithms that can learn good representations of the data and overcome OOM and TLE errors and moreover, improve the accuracy.

On the other hand, the traditional statistical methods located at the bottom of the table handle large workflows better since most of them do not consider structural information, which typically leads to OOM or TLE errors. However, their performance in terms of metrics is found to be poorer, with the best-performing method achieving a ROC-AUC value close to 0.6. It is worth noting that in binary scenarios, a ROC-AUC score below 0.5 indicates that the model’s performance is worse than random guessing, making it unsuitable for the task.

In summary, there is a clear need to develop novel methods to advance the state of the art and improve the performance of unsupervised learning methods on large, complex datasets.

Table 2: Model Comparison

|            | 1000 Genome |            |           | Montage |            |           | Predict Future Sales |            |           |
|------------|-------------|------------|-----------|---------|------------|-----------|----------------------|------------|-----------|
|            | ROC-AUC     | Ave. Prec. | Prec. @ k | ROC-AUC | Ave. Prec. | Prec. @ k | ROC-AUC              | Ave. Prec. | Prec. @ k |
| MLPAE      | .545        | .356       | .430      | .518    | .208       | .198      | .508                 | .120       | .153      |
| SCAN       | .491        | .323       | .274      | .500    | .204       | .230      | .500                 | .104       | .000      |
| Radar      |             | OOM        |           |         | OOM        |           | .632                 | .158       | .191      |
| Anomalous  |             | OOM        |           |         | OOM        |           | .607                 | .176       | .210      |
| GCNAE      | .610        | .38        | .426      | .519    | .211       | .146      | .398                 | .098       | .125      |
| Dominant   |             | OOM        |           |         | OOM        |           | .427                 | .089       | .112      |
| DONE       |             | OOM        |           |         | OOM        |           | .559                 | .130       | .143      |
| ADONE      |             | OOM        |           |         | OOM        |           | .579                 | .147       | .166      |
| AnomalyDAE |             | OOM        |           |         | OOM        |           | .584                 | .146       | .145      |
| GAAN       |             | OOM        |           |         | OOM        |           | .618                 | .160       | .175      |
| GUIDE      |             | TLE        |           |         | TLE        |           |                      | TLE        |           |
| CONAD      |             | TLE        |           |         | TLE        |           |                      | TLE        |           |
| ABOD       | .500        | .326       | .249      | .500    | .204       | .230      | .500                 | .104       | .000      |
| CBLOF      | .489        | .322       | .346      | .517    | .211       | .233      | .546                 | .119       | .182      |
| FB         | .509        | .330       | .297      | .487    | .201       | .205      | .451                 | .103       | .006      |
| HBOS       | .513        | .333       | .365      | .570    | .253       | .302      | .539                 | .116       | .169      |
| IF         | .504        | .328       | .357      | .497    | .204       | .209      | .560                 | .127       | .207      |
| KNN        | .558        | .374       | .384      | .566    | .250       | .297      | .663                 | .232       | .382      |
| AKNN       | .547        | .366       | .356      | .553    | .243       | .286      | .642                 | .224       | .327      |
| LOF        | .509        | .331       | .297      | .492    | .202       | .221      | .480                 | .102       | .058      |
| MCD        | .503        | .328       | .355      | .514    | .210       | .230      | .510                 | .106       | .117      |
| OCSVM      | .510        | .331       | .355      | .464    | .199       | .146      | .540                 | .117       | .172      |
| PCA        | .500        | .326       | .249      | .500    | .204       | .230      | .529                 | .112       | .152      |
| LSCP       | .494        | .324       | .289      | .490    | .202       | .206      | .530                 | .113       | .159      |
| INNE       | .503        | .328       | .350      | .461    | .200       | .145      | .466                 | .102       | .030      |
| GMM        | .486        | .321       | .341      | .502    | .205       | .203      | .532                 | .113       | .157      |
| KDE        | .514        | .334       | .357      |         | TLE        |           | .491                 | .103       | .084      |
| LMDD       |             | TLE        |           |         | TLE        |           | .557                 | .125       | .202      |

## 5 Generalization and Limitations

In this work, we provide three workflows, two of them corresponding to scientific applications and one of them corresponding to a data science workflow. While it is important to develop novel methods to facilitate unsupervised anomaly detection on these workflows, the use of these workflows in developing methods for a larger set of workflow anomaly detection problems is also relevant. Therefore, an important aspect of this work is the ability of the benchmark dataset to simulate anomalies across different scientific domains.

Since the workflow data is modeled as a DAG, it is feasible to use the ML methods that are developed to be precise on these workflows to work with other datasets that can be represented as DAG. Therefore, one may design approaches that can be built for anomaly detection for any application that generates data represented as a DAG including workflows that are not represented in this benchmark since a wide range of anomalies that can occur in real-world computational workflows.

Moreover, as we also provide the raw log data, researchers can use it to explore new methods and approaches for anomaly detection beyond the ones presented in this work. This can lead to the



development of more accurate and robust anomaly detection algorithms that can be applied to a wider range of computational workflows. For example, taking the context of the raw logs as inputs for natural language processing (NLP) tasks, such as large language models, can enable the development of more advanced anomaly detection algorithms that can capture the complex relationships between the various components of computational workflows, beyond the scope of graphs only capture the dependence between jobs.

Despite their usefulness, benchmark datasets with synthetic anomalies in computational workflows have some limitations. One limitation is that they may not fully capture the complexity and variability of real-world computational workflows. Scientific and data science workflows can be highly heterogeneous and may contain anomalies that are difficult to simulate using synthetic data. Another limitation is that benchmark datasets may not reflect the specific characteristics of the data in a particular scientific domain. Anomaly detection algorithms that perform well on benchmark datasets may not necessarily perform well on real-world data in a different scientific domain. Therefore, it is important to evaluate the performance of anomaly detection algorithms on real-world computational workflows in addition to benchmark datasets.

## 6 Conclusion

In this paper, we developed benchmark datasets for anomaly detection in computational workflows. Specifically, we have introduced a new dataset for benchmarking anomaly detection techniques, which includes systematically injected anomalies and raw execution logs from workflows executing on distributed infrastructures. We have also summarized the statistics of new datasets, as well as a set of open datasets, and provided insightful analyses.

Our benchmarking results show that unsupervised anomaly detection techniques can be effective for detecting anomalies in computational workflows. However, we also highlight the need for more research in this area, particularly in developing techniques that can handle the complexity and heterogeneity of computational workflows. We hope the study provides valuable insights into the challenges of anomaly detection in computational workflows and offers a starting point for future research in this area. We hope that our benchmark dataset and analysis will be useful for researchers and practitioners working on improving the reliability and reproducibility of computational workflows.

## Acknowledgments and Disclosure of Funding

This work is funded by the Department of Energy under the Integrated Computational and Data Infrastructure (ICDI) for Scientific Discovery, grant DE-SC0022328.

## References

- 1000 Genomes Project Consortium. A global reference for human genetic variation. *Nature*, 526(7571):68–74, 2012.
- Fabrizio Angiulli and Clara Pizzuti. Fast outlier detection in high dimensional spaces. In *Principles of Data Mining and Knowledge Discovery: 6th European Conference, PKDD 2002 Helsinki, Finland, August 19–23, 2002 Proceedings 6*, pages 15–27. Springer, 2002.
- Andreas Arning, Rakesh Agrawal, and Prabhakar Raghavan. A linear method for deviation detection in large databases. In *KDD*, volume 1141, pages 972–981, 1996.
- Inc. Association of Universities for Research in Astronomy. Digitized sky survey, 1994. URL <https://catcopy.ipac.caltech.edu/doi/doi.php?id=10.26131/IRSA441>.
- Tharindu R Bandaragoda, Kai Ming Ting, David Albrecht, Fei Tony Liu, Ye Zhu, and Jonathan R Wells. Isolation-based anomaly detection using nearest-neighbor ensembles. *Computational Intelligence*, 34(4): 968–998, 2018.
- Sambaran Bandyopadhyay, Saley Vishal Vivek, and MN Murty. Outlier resistant unsupervised deep architectures for attributed network embedding. In *Proceedings of the 13th international conference on web search and data mining*, pages 25–33, 2020.

- James Bergstra, Daniel Yamins, and David Cox. Making a science of model search: Hyperparameter optimization in hundreds of dimensions for vision architectures. In *International conference on machine learning*, pages 115–123. PMLR, 2013.
- Leo Breiman. Random forests. *Machine learning*, 45:5–32, 2001.
- Markus M Breunig, Hans-Peter Kriegel, Raymond T Ng, and Jörg Sander. Lof: identifying density-based local outliers. In *Proceedings of the 2000 ACM SIGMOD international conference on Management of data*, pages 93–104, 2000.
- S. Callaghan, P. J. Maechling, G. Juve, K. Vahi, E. Deelman, and T. H. Jordan. Optimizing CyberShake Seismic Hazard Workflows for Large HPC Resources. In *AGU Fall Meeting Abstracts*, volume 2014, pages IN21C–3720, December 2014.
- Tianqi Chen, Tong He, Michael Benesty, Vadim Khotilovich, Yuan Tang, Hyunsu Cho, Kailong Chen, Rory Mitchell, Ignacio Cano, Tianyi Zhou, et al. Xgboost: extreme gradient boosting. *R package version 0.4-2*, 1(4):1–4, 2015.
- Zhenxing Chen, Bo Liu, Meiqing Wang, Peng Dai, Jun Lv, and Liefeng Bo. Generative adversarial attributed network anomaly detection. In *Proceedings of the 29th ACM International Conference on Information & Knowledge Management*, pages 1989–1992, 2020.
- Ewa Deelman, Karan Vahi, Gideon Juve, Mats Rynge, Scott Callaghan, Philip J Maechling, Rajiv Mayani, Weiwei Chen, Rafael Ferreira da Silva, Miron Livny, and Kent Wenger. Pegasus: a workflow management system for science automation. *Future Generation Computer Systems*, 46:17–35, 2015. doi: 10.1016/j.future.2014.10.008.
- Ewa Deelman, Christopher Carothers, Anirban Mandal, Brian Tierney, Jeffrey S Vetter, Ilya Baldin, Claris Castillo, Gideon Juve, Dariusz Król, Vickie Lynch, et al. Panorama: An approach to performance modeling and diagnosis of extreme-scale workflows. *The International Journal of High Performance Computing Applications*, 31(1):4–18, 2017.
- Kaize Ding, Jundong Li, Rohit Bhanushali, and Huan Liu. Deep anomaly detection on attributed networks. In *Proceedings of the 2019 SIAM International Conference on Data Mining*, pages 594–602. SIAM, 2019.
- Docker Inc. Docker. <https://docs.docker.com/>, 2022.
- ELK Stack, 2018. ELK stack. <https://www.elastic.co/elk-stack>, 2018.
- Haoyi Fan, Fengbin Zhang, and Zuoyong Li. Anomalydae: Dual autoencoder for anomaly detection on attributed networks. In *ICASSP 2020-2020 IEEE International Conference on Acoustics, Speech and Signal Processing (ICASSP)*, pages 5685–5689. IEEE, 2020.
- Matthias Fey and Jan E. Lenssen. Fast graph representation learning with PyTorch Geometric. In *ICLR Workshop on Representation Learning on Graphs and Manifolds*, 2019.
- Markus Goldstein. Special issue on unsupervised anomaly detection, 2023.
- Markus Goldstein and Andreas Dengel. Histogram-based outlier score (hbos): A fast unsupervised anomaly detection algorithm. *KI-2012: poster and demo track*, 1:59–63, 2012.
- William L Hamilton, Rex Ying, and Jure Leskovec. Inductive representation learning on large graphs. In *Proceedings of NIPS*, 2017.
- Johanna Hardin and David M Rocke. Outlier detection in the multiple cluster setting using the minimum covariance determinant estimator. *Computational Statistics & Data Analysis*, 44(4):625–638, 2004.
- Zengyou He, Xiaofei Xu, and Shengchun Deng. Discovering cluster-based local outliers. *Pattern recognition letters*, 24(9-10):1641–1650, 2003.
- Marti A. Hearst, Susan T Dumais, Edgar Osuna, John Platt, and Bernhard Scholkopf. Support vector machines. *IEEE Intelligent Systems and their applications*, 13(4):18–28, 1998.
- HTCondor, 2023. Htcondor, 2023.
- Joseph C. Jacob, Daniel S. Katz, G. Bruce Berriman, John Good, Anastasia C. Laity, Ewa Deelman, Carl Kesselman, Gurmeet Singh, Mei-Hui Su, Thomas A. Prince, and Roy Williams. Montage: An Astronomical Image Mosaicking Toolkit. *Astrophysics Source Code Library*, record ascl:1010.036, October 2010.

- Kaggle. <https://www.kaggle.com/c/competitive-data-science-predict-future-sales>, 2020.
- Kate Keahey, Jason Anderson, Zhuo Zhen, Pierre Riteau, Paul Ruth, Dan Stanzione, Mert Cevik, Jacob Colleran, Haryadi S. Gunawi, Cody Hammock, Joe Mambretti, Alexander Barnes, François Halbach, Alex Rocha, and Joe Stubbs. Lessons learned from the chameleon testbed. In *Proceedings of the 2020 USENIX Annual Technical Conference (USENIX ATC '20)*. USENIX Association, July 2020.
- Linux Kernel. <https://www.kernel.org/doc/html/latest/admin-guide/cgroup-v2.html>, 2015.
- Thomas N Kipf and Max Welling. Variational graph auto-encoders. *arXiv preprint arXiv:1611.07308*, 2016.
- Hans-Peter Kriegel, Matthias Schubert, and Arthur Zimek. Angle-based outlier detection in high-dimensional data. In *Proceedings of the 14th ACM SIGKDD international conference on Knowledge discovery and data mining*, pages 444–452, 2008.
- Longin Jan Latecki, Aleksandar Lazarevic, and Dragoljub Pokrajac. Outlier detection with kernel density functions. In *MLDM*, volume 7, pages 61–75, 2007.
- Aleksandar Lazarevic and Vipin Kumar. Feature bagging for outlier detection. In *Proceedings of the eleventh ACM SIGKDD international conference on Knowledge discovery in data mining*, pages 157–166, 2005.
- Jundong Li, Harsh Dani, Xia Hu, and Huan Liu. Radar: Residual analysis for anomaly detection in attributed networks. In *IJCAI*, volume 17, pages 2152–2158, 2017.
- Fei Tony Liu, Kai Ming Ting, and Zhi-Hua Zhou. Isolation forest. In *2008 eighth ieee international conference on data mining*, pages 413–422. IEEE, 2008.
- Kay Liu, Yingdong Dou, Yue Zhao, Xueying Ding, Xiyang Hu, Ruitong Zhang, Kaize Ding, Canyu Chen, Hao Peng, Kai Shu, Lichao Sun, Jundong Li, George H. Chen, Zhihao Jia, and Philip S. Yu. Bond: Benchmarking unsupervised outlier node detection on static attributed graphs. *Advances in Neural Information Processing Systems*, 35:27021–27035, 2022.
- Stuart Lloyd. Least squares quantization in pcm. *IEEE transactions on information theory*, 28(2):129–137, 1982.
- Zhi Ma, Yaozhi Luo, Chung-Bang Yun, Hua-Ping Wan, and Yanbin Shen. An mppca-based approach for anomaly detection of structures under multiple operational conditions and missing data. *Structural Health Monitoring*, 22(2):1069–1089, 2023.
- Alexander H. Nitz, Thomas Dent, Tito Dal Canton, Stephen Fairhurst, and Duncan A. Brown. Detecting binary compact-object mergers with gravitational waves: Understanding and improving the sensitivity of the pycbc search. *The Astrophysical Journal*, 849(2):118, nov 2017. doi: 10.3847/1538-4357/aa8f50. URL <https://dx.doi.org/10.3847/1538-4357/aa8f50>.
- Adam J. Oliner and Jon Stearley. What supercomputers say: A study of five system logs. In *The 37th Annual IEEE/IFIP International Conference on Dependable Systems and Networks, DSN 2007, 25-28 June 2007, Edinburgh, UK, Proceedings*, pages 575–584. IEEE Computer Society, 2007. doi: 10.1109/DSN.2007.103. URL <https://doi.org/10.1109/DSN.2007.103>.
- George Papadimitriou, Cong Wang, Karan Vahi, Rafael Ferreira da Silva, Anirban Mandal, Zhengchun Liu, Rajiv Mayani, Mats Rynge, Mariam Kiran, Vickie E Lynch, et al. End-to-end online performance data capture and analysis for scientific workflows. *Future Generation Computer Systems*, 117:387–400, 2021.
- Zhen Peng, Minnan Luo, Jundong Li, Huan Liu, Qinghua Zheng, et al. Anomalous: A joint modeling approach for anomaly detection on attributed networks. In *IJCAI*, pages 3513–3519, 2018.
- J. Ross Quinlan. Induction of decision trees. *Machine learning*, 1:81–106, 1986.
- Sridhar Ramaswamy, Rajeev Rastogi, and Kyuseok Shim. Efficient algorithms for mining outliers from large data sets. In *Proceedings of the 2000 ACM SIGMOD international conference on Management of data*, pages 427–438, 2000.
- Carl Rasmussen. The infinite gaussian mixture model. *Advances in neural information processing systems*, 12, 1999.
- Mayu Sakurada and Takehisa Yairi. Anomaly detection using autoencoders with nonlinear dimensionality reduction. In *Proceedings of the MLSDA 2014 2nd workshop on machine learning for sensory data analysis*, pages 4–11, 2014.

- Bernhard Schölkopf, John C Platt, John Shawe-Taylor, Alex J Smola, and Robert C Williamson. Estimating the support of a high-dimensional distribution. *Neural computation*, 13(7):1443–1471, 2001.
- SciTech, 2017. Pegasus panorama. <https://github.com/pegasus-isi/pegasus/tree/panorama>.
- Mei-Ling Shyu, Shu-Ching Chen, Kanoksri Sarinnapakorn, and LiWu Chang. A novel anomaly detection scheme based on principal component classifier. Technical report, Miami Univ Coral Gables Fl Dept of Electrical and Computer Engineering, 2003.
- Kihyuk Sohn, Jinsung Yoon, Chun-Liang Li, Chen-Yu Lee, and Tomas Pfister. Anomaly clustering: Grouping images into coherent clusters of anomaly types. In *Proceedings of the IEEE/CVF Winter Conference on Applications of Computer Vision*, pages 5479–5490, 2023.
- Petar Velickovic, Guillem Cucurull, Arantxa Casanova, Adriana Romero, Pietro Lio, and Yoshua Bengio. Graph attention networks. In *International conference on learning representations*, 2018.
- Xiaowei Xu, Nurcan Yuruk, Zhidan Feng, and Thomas AJ Schweiger. Scan: a structural clustering algorithm for networks. In *Proceedings of the 13th ACM SIGKDD international conference on Knowledge discovery and data mining*, pages 824–833, 2007.
- Zhiming Xu, Xiao Huang, Yue Zhao, Yushun Dong, and Jundong Li. Contrastive attributed network anomaly detection with data augmentation. In *Advances in Knowledge Discovery and Data Mining: 26th Pacific-Asia Conference, PAKDD 2022, Chengdu, China, May 16–19, 2022, Proceedings, Part II*, pages 444–457. Springer, 2022.
- Xu Yuan, Na Zhou, Shuo Yu, Huafei Huang, Zhikui Chen, and Feng Xia. Higher-order structure based anomaly detection on attributed networks. In *2021 IEEE International Conference on Big Data (Big Data)*, pages 2691–2700. IEEE, 2021.
- Yue Zhao, Zain Nasrullah, Maciej K Hryniewicki, and Zheng Li. Lscp: Locally selective combination in parallel outlier ensembles. In *Proceedings of the 2019 SIAM International Conference on Data Mining*, pages 585–593. SIAM, 2019a.
- Yue Zhao, Zain Nasrullah, and Zheng Li. Pyod: A python toolbox for scalable outlier detection. *Journal of Machine Learning Research*, 20(96):1–7, 2019b. URL <http://jmlr.org/papers/v20/19-011.html>.

## Appendix

Flow-Bench code and data repository: <https://github.com/PoSeiDon-Workflows/flowbench>

### A Workflow Diagrams

Figure 3, 4 and 5 are the workflow diagrams of the 1000 Genome, Montage and Predict Future Sales workflows, respectively.

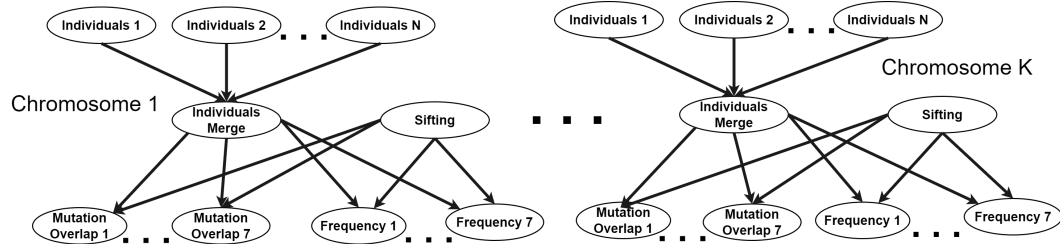


Figure 3: Overview of the 1000Genome sequencing analysis workflow. The workflow creates a branch for each chromosome and each individual task is processing a subset of the Phase 3 data (equally distributed).

### B Parsed Features

Table 3 shows the features that are parsed from the Pegasus workflow logs, with the type of each feature and a brief description.

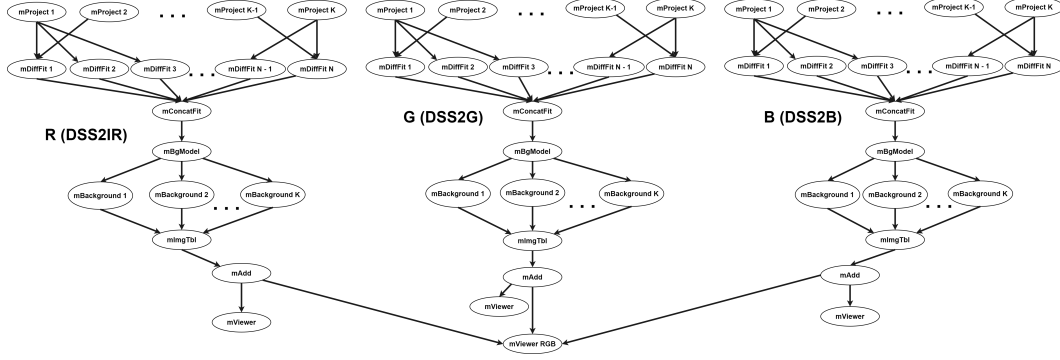


Figure 4: Overview of the Montage workflow. In this case, the workflow uses images captured by the Digitized Sky Survey (DSS) [Association of Universities for Research in Astronomy, 1994] and creates a branch for each band that is requested to be processed during the workflow generation. The size of the first level of each branch depends on the size of the section of the sky to be analyzed, while the second level on the number of overlapping images stored in the archive.

Table 3: Parsed Dataset Features.

| Field                                     | Data Type | Description   |
|---|-----------|---|
| node_id                                   | string    | Exec. DAG Node ID   |
| anomaly_type                              | string    | Anomaly label   |
| type                                      | int       | Pegasus job type  |
| is_clustered                              | int       | 1 if job clustering enabled else 0  |
| ready                                     | ts        | Epoch ts when all dependencies have been met and job can be dispatched                            |
| pre_script_start                          | ts        | Epoch ts when the pre-script started executing  |
| pre_script_end                            | ts        | Epoch ts when the pre-script stopped executing  |
| submit                                    | ts        | Epoch ts when the job was submitted to the queue  |
| stage_in_start                            | ts        | Epoch ts when the data stage in started   |
| stage_in_end                              | ts        | Epoch ts when the data stage in ended   |
| stage_in_effective_bytes_per_sec          | float     | Bytes written per second (input data)   |
| execute_start                             | ts        | Epoch ts when the execution starts  |
| execute_end                               | ts        | Epoch ts when the execution ends  |
| stage_out_start                           | ts        | Epoch ts when the data stage out started  |
| stage_out_end                             | ts        | Epoch ts when the data stage out ended  |
| stage_out_effective_bytes_per_sec         | float     | Bytes written per second (output data)  |
| post_script_start                         | ts        | Epoch ts when the post-script started executing   |
| post_script_end                           | ts        | Epoch ts when the post-script ended executing   |
| wms_delay                                 | float     | Composite field estimating the delay introduced by the WMS while preparing the job for submission |
| pre_script_delay                          | float     | Composite field estimating the delay introduced by the pre-script                                 |
| queue_delay                               | float     | Composite field estimating the time spent in the queue  |
| runtime                                   | float     | Total runtime of the job, based on execute start and end  |
| post_script_delay                         | float     | Composite field estimating the delay introduced by the post-script                                |
| stage_in_delay                            | float     | Total time spend staging in data, based on stage in start and end                                 |
| stage_in_bytes                            | float     | Total bytes staged in   |
| stage_out_delay                           | float     | Total time spend staging out data, based on stage out start and end                               |
| stage_out_bytes                           | float     | Total bytes staged out  |
| kickstart_user                            | string    | Name of the user submitted the job  |
| kickstart_site                            | string    | Name of the execution site  |
| kickstart_hostname                        | string    | Hostname of the worker node the job executed on   |
| kickstart_transformations                 | string    | Mapping of the executable locations   |
| kickstart_executables                     | string    | Names of the invoked executables  |
| kickstart_executables_argv                | string    | Command line arguments used to invoke the executables   |
| kickstart_executables_cpu_time            | float     | Total cpu time  |
| kickstart_status                          | int       | The status of the job as marked by Pegasus Kickstart  |
| kickstart_executables_exitcode            | int       | The exitcode of the invoked executable(s)   |
| kickstart_online_iowait                   | float     | Time spent on waiting for io (seconds)  |
| kickstart_online_bytes_read               | float     | Total bytes read from disk (bytes)  |
| kickstart_online_bytes_written            | float     | Total bytes written to disk (bytes)   |
| kickstart_online_read_system_calls        | float     | Number of read system calls   |
| kickstart_online_write_system_calls       | float     | Number of write system calls  |
| kickstart_online_untime                   | float     | Time spent on user space  |
| kickstart_online_stime                    | float     | Time spent on kernel space  |
| kickstart_online_bytes_read_per_second    | float     | Bytes read per second (effective)   |
| kickstart_online_bytes_written_per_second | float     | Bytes written per second (effective)  |

## C Benchmark algorithms

Table 4 provide the selected benchmark algorithms and their references. The input  $X$  represents using features only, while  $A, X$  represents using both structure and features.

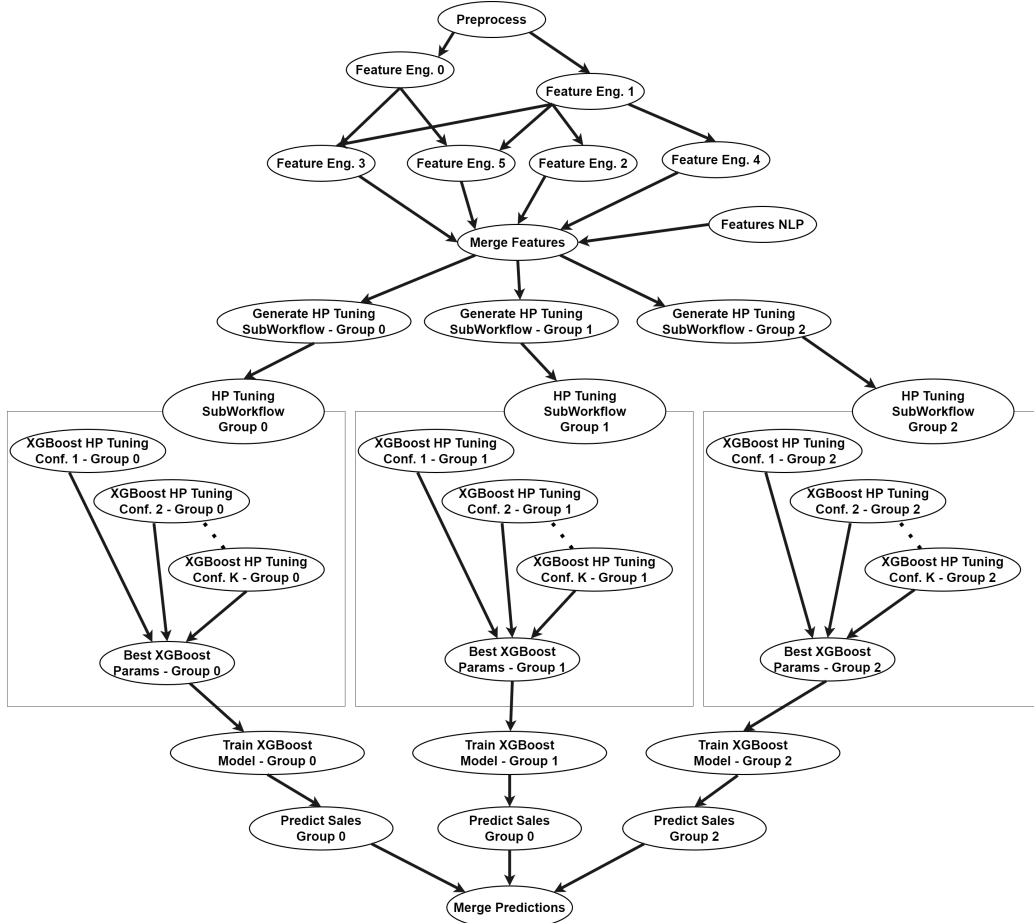


Figure 5: Overview of the Predict Future Sales workflow. The workflow splits the data into 3 item categories and trains 3 XGBoost models that are later combined, using an ensemble technique. It contains 3 hyperparameter tuning subworkflows, that test different sets of features and picks the best performing one. The number of HPO tasks is configurable and depends on the number of combinations that will be tested.

## D Data processing

Followed by Table 3, we further processed the parsed data into a dataset in PyTorch-Geometric (PyG) format [Fey and Lenssen, 2019] for the graph-based algorithms. The PyG format is a standard format for graph data in deep learning, which is widely used in the graph neural network (GNN) community. The PyG format is a tuple of  $(\mathbf{X}, \mathbf{A}, \mathbf{y})$ , where  $\mathbf{X}$  is the feature matrix,  $\mathbf{A}$  is the adjacency matrix, and  $\mathbf{y}$  is the label vector. First, for the features with integers/strings as categories, we processed them into one-hot encoding, and then concatenate them into a feature vector  $\mathbf{X}$ . Notice that there are multiple features with timestamps, we shifted the timestamp to the same starting point (i.e., the first timestamp in the dataset), which allows us to measure the behavior of each individual job independently. Moreover, we normalized job feature column-wise, in which we use min-max normalization such that normalized features are in the range  $[0, 1]$ . Second, for the structural information, we convert the dependencies as directed edges between nodes, and furthermore, we convert the directed acyclic graphs into undirected graphs as  $\mathbf{A}$ . Finally, we use the label vector  $\mathbf{y}$  to indicate job anomalies, where 1 indicates anomalous jobs and 0 indicates normal jobs. For the experiment in the paper, we split the dataset into training, validation, and test set with a ratio 0.6, 0.2, and 0.2, and use the dataloader to load the dataset in mini-batch for training. All the steps are built into a pipeline as the transform class in PyG, which allows us to easily process the dataset into PyG format.

Table 4: Selected algorithms for anomaly detection. The input  $X$  represents using features only, while  $A, X$  represents using both structure and features.

| Algorithm  | Reference                   | Input Data | ML Supervision | Backbone          |
|------------|-----------------------------|------------|----------------|-------------------|
| ABOD       | Kriegel et al. [2008]       | X          | Unsupervised   | Probabilistic     |
| CBLOF      | He et al. [2003]            | X          | Unsupervised   | Neighbors         |
| FB         | Lazarevic and Kumar [2005]  | X          | Unsupervised   | Ensembles         |
| HBOS       | Goldstein and Dengel [2012] | X          | Unsupervised   | Neighbors         |
| IF         | Liu et al. [2008]           | X          | Unsupervised   | Ensembles         |
| KNN        | Ramaswamy et al. [2000]     | X          | Unsupervised   | Neighbors         |
| AKNN       | Angiulli and Pizzuti [2002] | X          | Unsupervised   | Neighbors         |
| LOF        | Breunig et al. [2000]       | X          | Unsupervised   | Neighbors         |
| MCD        | Hardin and Rocke [2004]     | X          | Unsupervised   | Linear            |
| OCSVM      | Schölkopf et al. [2001]     | X          | Unsupervised   | Linear            |
| PCA        | Shyu et al. [2003]          | X          | Unsupervised   | Decomposition     |
| LSCP       | Zhao et al. [2019a]         | X          | Unsupervised   | Ensembles         |
| INNE       | Bandaragoda et al. [2018]   | X          | Unsupervised   | Ensembles         |
| GMM        | Rasmussen [1999]            | X          | Unsupervised   | Mixture           |
| KDE        | Latecki et al. [2007]       | X          | Unsupervised   | Probabilistic     |
| LMDD       | Arning et al. [1996]        | X          | Unsupervised   | Linear            |
| MLPAE      | Sakurada and Yairi [2014]   | X          | Unsupervised   | MLP, AE           |
| SCAN       | Xu et al. [2007]            | A, X       | Unsupervised   | Clustering        |
| Radar      | Li et al. [2017]            | A, X       | Unsupervised   | Decomposition     |
| Anomalous  | Peng et al. [2018]          | A, X       | Unsupervised   | Decomposition     |
| GCNAE      | Kipf and Welling [2016]     | A, X       | Unsupervised   | GNN, Auto-encoder |
| Dominant   | Ding et al. [2019]          | A, X       | Unsupervised   | GNN, Auto-encoder |
| DONE       | Bandyopadhyay et al. [2020] | A, X       | Unsupervised   | MLP, Auto-encoder |
| ADONE      | Bandyopadhyay et al. [2020] | A, X       | Unsupervised   | MLP, Auto-encoder |
| AnomalyDAE | Fan et al. [2020]           | A, X       | Unsupervised   | GNN, Auto-encoder |
| GAAN       | Chen et al. [2020]          | A, X       | Unsupervised   | GAN               |
| GUIDE      | Yuan et al. [2021]          | A, X       | Unsupervised   | GNN, Auto-encoder |
| CONAD      | Xu et al. [2022]            | A, X       | Unsupervised   | GNN, Auto-encoder |

## E Detailed benchmark settings for algorithms

Following in Table 4, we provide the detailed settings for each algorithm used in the benchmark. Notice that we use the default settings for all the algorithms, and we do not tune the hyperparameters for each algorithm. For the hyperparameters that are not listed below, we use the default settings in the implementation of each algorithm from PyOD and PyGOD.

- **ABOD.** N/A.
- **CBLOF.** Check estimator: False.
- **FB.** Number of neighbors: 35.
- **HBOS.** N/A.
- **IF.** N/A.
- **KNN.** N/A.
- **AKNN.** Aggregation method: average.
- **LOF.** Number of neighbors: 35.
- **MCD.** N/A.
- **OCSVM.** N/A.
- **PCA.** N/A.
- **LSCP.** Detector list with a set of LOF models on a number of neighbors: 5, 10, 15, 20, 25, 30, 35, 40, 45, 50.
- **INNE.** Max samples: 2.
- **GMM.** N/A.
- **KDE.** N/A.
- **LMDD.** N/A.

- **MLPAE**. Hidden dimension: 64, batch size: 64 learning rate: 1e-3, weight decay: 1e-5, dropout: 0.5, epochs: 200.
- **SCAN**.  $\epsilon = 0.5$ ,  $\mu = 5$ .
- **Radar**. Learning rate: 1e-3.
- **Anomalous**. Learning rate: 1e-3.
- **GCNAE**. Hidden dimension: 64, batch size: 64 learning rate: 1e-3, weight decay: 1e-5, dropout: 0.5, epochs: 200.
- **Dominant**. Hidden dimension: 64, batch size: 64 learning rate: 1e-3, weight decay: 1e-5, dropout: 0.5, epochs: 200.
- **DONE**. Hidden dimension: 64, batch size: 64 learning rate: 1e-3, weight decay: 1e-5, dropout: 0.5, epochs: 200.
- **ADONE**. Hidden dimension: 64, batch size: 64 learning rate: 1e-3, weight decay: 1e-5, dropout: 0.5, epochs: 200.
- **AnomalyDAE**. Hidden dimension: 64, batch size: 64 learning rate: 1e-3, weight decay: 1e-5, dropout: 0.5, epochs: 200,  $\alpha = 0.5$ ,  $\theta = 10$ ,  $\eta = 5$ .
- **GAAN**. Hidden dimension: 64, batch size: 64 learning rate: 1e-3, weight decay: 1e-5, dropout: 0.5, epochs: 200.
- **GUIDE**. Feature hidden dimension: 64, structure hidden dimension: 5, batch size: 64 learning rate: 1e-3, weight decay: 1e-5, dropout: 0.5, epochs: 200.
- **CONAD**. Hidden dimension: 64, batch size: 64 learning rate: 1e-3, weight decay: 1e-5, dropout: 0.5, epochs: 200.